Destabilization of a self-trapped exciton in a quasi-one-dimensional semiconductor: $Mg[Pt(CN)_4]\cdot 7H_2O$ with hydrostatic pressure

U. Rössler
Institut für Theoretische Physik, Universität Regensburg, D-8400 Regensburg, Germany

H. Yersin
Institut für Physikalische und Theoretische Chemie, Universität Regensburg, D-8400 Regensburg, Germany

(Received 21 April 1982)

Optical data from single-crystal $Mg[Pt(CN)_4]\cdot 7H_2O$ together with calculations of the exciton energies allow us to draw conclusions on the existence of a self-trapped exciton, which becomes metastable by changing the relevant material parameters with hydrostatic pressure.

An exciton in a deformable lattice is in a stable localized (self-trapped) state if the exciton-lattice interaction is stronger than the energy transfer between lattice sites; otherwise, the stable exciton state is delocalized.[1] The relative strengths of exciton-lattice interaction and energy transfer depend on the material parameters, which in a continuum model are the exciton mass, the deformation potential, and the elastic constants. By a proper change of these parameters it is conceivable to destabilize a self-trapped exciton (STE). An efficient variation of the intrinsic material constants is possible in the highly anisotropic (quasi-one-dimensional) semiconductor[2-4] $Mg[Pt(CN)_4]\cdot 7H_2O$ by the application of hydrostatic pressure. Optical emission spectra of this system together with calculations of the exciton energies give evidence that due to stress-induced alteration of the intrinsic parameters a STE is destabilized. The high anisotropy (quasi-one-dimensionality) of $Mg[Pt(CN)_4]\cdot 7H_2O$ seems to be crucial for this effect which, to our knowledge, has not been observed so far in other solids.

The fundamental optical transition energies of $M_x[Pt(CN)_4]\cdot nH_2O$, which for different cations M and crystal water content n can be varied from the uv to the red spectral region, are correlated with the in-chain metal-metal distance R.[5-8] In particular, for $Mg[Pt(CN)_4]\cdot 7H_2O$ with $R = 3.155$ Å these transition peak energies are 19 400 cm^{-1} from reflectivity data and 17 600 cm^{-1} from emission spectra (at 295 K). The Pt-Pt distance R can be further decreased by hydrostatic pressure and becomes for $Mg[Pt(CN)_4]\cdot 7H_2O$, at about 20 kbar, $R \approx 3.0$ Å^3 with optical transition energies of about 13 300 cm^{-1} in reflectivity and 11 800 cm^{-1} in emission. Calculations for the $[Pt(CN)_4]^{2-}$ dimer demonstrate the strong overlap of Pt $6p_z$ (hybridized with ligand $CN\pi^*$ orbitals) and of Pt $5d_{z^2}, 6s$ orbitals on neighboring complexes.[9] As a consequence one expects the formation of energy bands for the periodic structure.[10] In fact, it is possible to ascribe the R dependence of the optical data to a decrease of the energy gap between the conduction band, which originates mainly from (Pt $6p_z$, $CN\pi^*$) orbitals, and the (Pt $5d_{z^2}, 6s$) valence band with decreasing R.[11]

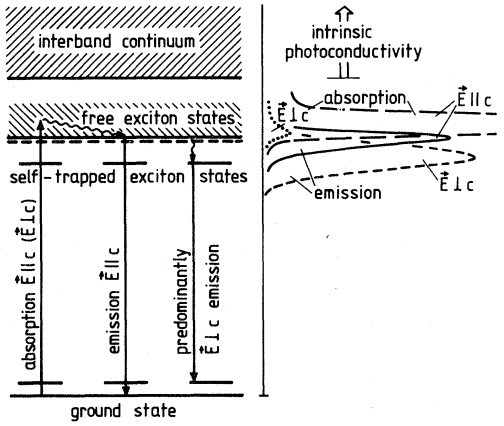

FIG. 1. Phenomenological energy-level diagram for the lowest electronic states and schematic (simplified) optical spectra of tetracyanoplatinates (II).

The available information on the nature of the excited electron states is summarized in the phenomenological energy-level diagram for tetracyanoplatinates in Fig. 1.[6,7] The optical absorption is highly polarized with the electric field vector $\vec{E}||c$ (c being the chain axis), as is expected from the symmetry of the valence-band edge (a_{1g}) and the conduction-band edge (a_{2u}) in the crystal-point group D_{4h}. The details of the optical spectra (Fig. 1) can be understood only by including spin and correlation effects. The electronic ground state has A'_{1g} symmetry in double-group notation of D'_{4h} ($^1A_{1g}$ in single group D_{4h}) while the lowest excited states have symmetry A'_{2u} ($^1A_{2u}$) (allowed for $\vec{E}||c$), E'_u ($^3A_{2u}$) (allowed for $\vec{E}\perp c$), and A'_{1u} ($^3A_{2u}$) (dipole forbidden). Since the oscillator strength of the $\vec{E}||c$ transition is close to one, it is ascribed to a delocalized exciton, being mainly of singlet character A'_{2u}. The emission from this state, whose lifetime of $\tau<0.3\times10^{-9}$ s at 1.7 K (Ref. 12) is consistent with the oscillator strength of the $\vec{E}||c$ absorption, is observed with a slight red shift due to reabsorption. The interpretation as a delocalized exciton is supported by photoconductivity[13] and doping experiments.[14] The $\vec{E}\perp c$ absorption observed at the low energetic rise of the $\vec{E}||c$ absorption has an oscillator strength of the order of 10^{-3}. It is ascribed to the delocalized triplet exciton E'_u ($^3A_{2u}$) which is weakly allowed due to spin-orbit coupling.[6,7]

At lower energy optical transitions are possible, which can be detected only in emission (mainly $\vec{E}\perp c$) with longer lifetime. The red shift of this emission against the short-living $\vec{E}||c$ emission decreases with decreasing R over the whole spectral range.[5–7] For $Mg[Pt(CN)_4]\cdot7H_2O$ at hydrostatic pressure of about 13 kbar (corresponding to R between 3.05 and 3.00 Å at 295 K) the $\vec{E}\perp c$ emission vanishes.[5] Moreover, doping experiments prove that this emission is intrinsic and a series of experimental facts indicate that the corresponding electronic states are localized to a few planar $[Pt(CN)_4]^{2-}$ complexes within a chain. Some of these experimental facts are the following:

(i) A small $[Ni(CN)_4]^{2-}$ impurity concentration quenches selectively the $\vec{E}\perp c$ emission. The temperature behavior is explained by a phonon-assisted hopping between localized states and the quencher.[14]

(ii) The $\vec{E}\perp c$ emission lifetime is reduced by rare-earth impurities and at low temperatures one observes a two-component decay. The long-living component equals the intrinsic one and the short-living component is attributed to regions, emitting near the impurities.[7,12,15]

(iii) A blue shift of about 270 cm^{-1} (corresponding to a $[Pt(CN)_4]^{2-}$ vibration) observed in the $\vec{E}\perp c$ emission under high magnetic fields is explained by assuming a localized state.[15]

(iv) An exchange of the crystal water H_2O to D_2O strongly increases the $\vec{E}\perp c$ emission intensity. This behavior is expected for localized states which are coupled to the water vibrations.[7]

Owing to the translational symmetry of the crystal, even a localized intrinsic electron state forms an energy band. Emission data from doped material[14,15] allow us to give a rough estimate of the *upper limit* for the bandwidth; the intrinsic emission (at 25 K) starts to decrease at an impurity concentration $x\simeq10^{-3}$, which means that the characteristic capture time by impurities becomes comparable with the intrinsic recombination lifetime ($\tau\approx3\times10^{-6}$ s at 25 K). If one considers only one-dimensional hopping an impurity site is reached after 10^6 steps (for $x=10^{-3}$).[7,16] This gives a lower limit for the resting time Δt at one $[Pt(CN)_4]^{2-}$ unit of about 3×10^{-12} s and, consequently, an upper limit of the bandwidth $\Delta\epsilon\approx\hbar/\Delta t$ of about 2 cm^{-1} (~0.25 meV). Because $\Delta\epsilon$ is at least a factor of 10^4 smaller than the calculated widths of conduction and valence bands,[10,11] there must be a very efficient intrinsic localization mechanism which most likely is the electron-lattice interaction. Therefore, we interpret the excited electron state responsible for the $\vec{E}\perp c$ emission as STE. If there is no symmetry-lowering lattice distortion, the symmetry classification of the STE is the same as for the delocalized free ex-

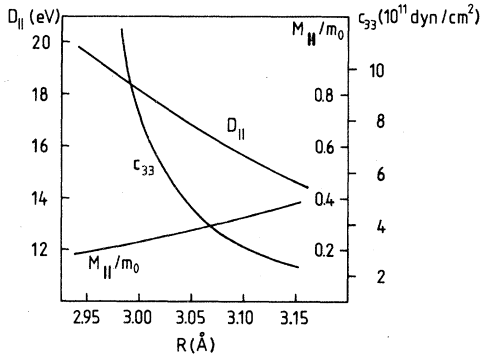

FIG. 2. R-dependent longitudinal input parameters for calculations of the total energy [Eq. (2) with Eq. (5)]: $M_{||}=m_{e||}+m_{h||}$ is the exciton mass, $D_{||}$ the deformation potential, and c_{33} the elastic constant. R is the in-chain metal-metal distance between neighboring $[Pt(CN)_4]$ complexes.

citon, i.e., it consists of components with symmetry A'_{2u} ($^1A_{2u}$) ($\vec{E}||c$), E'_u ($^3A_{2u}$) ($\vec{E}\perp c$), and A'_{1u} ($^3A_{2u}$), whose separation is larger than for the free exciton, since exchange effects increase due to localization. Though emission from all these localized states has been detected[7,15] the emission via the E'_u state is dominant due to exchange splitting and relaxation.

To confirm the phenomenological energy-level diagram of Fig. 1 and the R-dependent kinetic features of the different excited electron states, we started from the band model[11] and considered the effects of electron-hole and of electron-phonon interaction in the case of high anisotropy[17,18] within a continuum model. The band calculations[11] with the input parameters of Ref. 10 yield the energy gap (E_g), the longitudinal masses of electron ($m_{e||}$) and hole ($m_{h||}$), and the deformation potential $D_{||}=\Delta E_g/(\Delta R/R)$ as a function of R (Figs. 2 and 3). Of the dielectric constants, which are required in the calculations of the exciton binding energy[17] E_b, $\epsilon_{\infty||}$ has been determined from

$$\epsilon_{\infty||}=1+\frac{\gamma}{RE_g^2(R)} \tag{1}$$

with the calculated values for $E_g(R)$. The parameter γ and the optical constants $\epsilon_{\infty\perp}=2.5$, $\epsilon_{0\perp}=3.5$, and $\epsilon_{0||}=\epsilon_{\infty||}+1$ were chosen independent of R and according to available data for

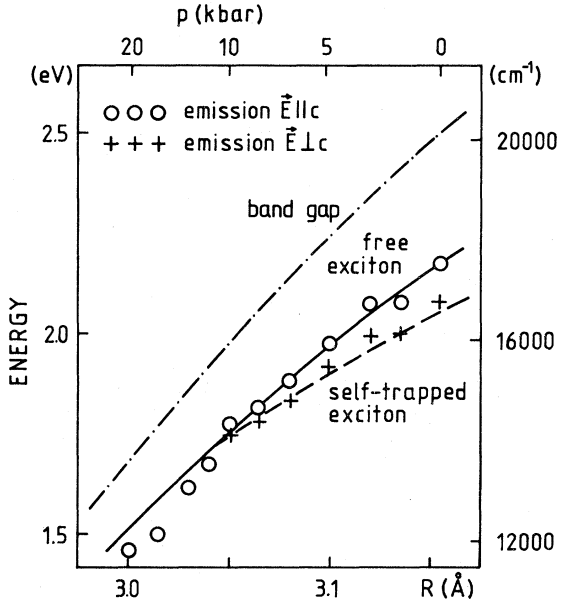

FIG. 3. Comparison between the R dependence of polarized emission for $Mg[Pt(CN)_4]\cdot 7H_2O$ (Ref. 5) and calculations for the energy gap, free-exciton energy, and self-trapped exciton energy.

$Ba[Pt(CN)_4]\cdot 4H_2O$.[19] The transverse electron and hole masses $m_{e\perp}=1.3m_0$ and $m_{h\perp}=1.75m_0$, which are not expected to depend on R, were chosen to reproduce the experimental binding energy for $Ba[Pt(CN)_4]\cdot 4H_2O$ as obtained from photoconductivity experiments. The R-dependent exciton energies are given in Fig. 3; they correspond closely to the transition energies of the $\vec{E}||c$ emission.

The stability of delocalized and self-trapped states depends on the total energy of the exciton (kinetic energy), the lattice deformation, and the exciton-lattice interaction as a functional of the exciton envelope.[1] For an exciton in an anisotropic elastic continuum this energy is[18]

$$E(\alpha_\perp,\alpha_{||})=\frac{\hbar^2\pi}{2M_\perp}\left[2\frac{\alpha_\perp^2}{a_\perp^2}+\frac{M_\perp}{M_{||}}\frac{\alpha_{||}^2}{a_{||}^2}\right] -E_{\rm ac}\frac{\alpha_\perp^2}{a_\perp^2}\frac{\alpha_{||}}{a_{||}}, \tag{2}$$

where $M=m_e+m_h$ is the total mass of the exciton and a is the lattice constant. $\alpha_{||}$ and $\alpha_\perp$ characterize the localization parallel and perpendicular to the chain of the exciton-envelope function which is assumed as an anisotropic Gaussian

$$\psi(\vec{r})=2^{3/4}\frac{(\alpha_\perp\alpha_{||})^{1/2}}{(a_\perp a_{||})^{1/2}} \times\exp\left[-\pi\left[\frac{\alpha_\perp^2}{a_\perp^2}(x^2+y^2)+\frac{\alpha_{||}^2}{a_{||}^2}z^2\right]\right]. \tag{3}$$

The elastic deformation-energy parameter

$$E_{\rm ac}=\frac{c_{33}D_\perp^2-4c_{13}D_\perp D_{||}+2(c_{11}+c_{12})D_{||}^2}{4[c_{33}(c_{11}+c_{12})-2c_{13}^2]} \tag{4}$$

depends on the elastic constants c_{ij} and on deformation potentials D. Comparison of optical data for tetracyanoplatinates with different transverse lattice constants but same R allows us to give an upper limit of $D_\perp<0.3$ eV $\ll D_{||}$ (see Fig. 2). Thus assuming $c_{33}\gg c_{13}$, Eq. (4) reduces to

$$E_{\rm ac}=\frac{1}{2}\frac{D_{||}^2}{c_{33}}, \tag{5}$$

where $c_{33}(R)$ can be determined from compressibility data[3] (Fig. 2).

The total energy $E(\alpha_{||},\alpha_\perp)$ of Eq. (2) can be visualized in an energy contour diagram as given in the inset of Fig. 4. It represents a generalization of the total-energy expression for the isotropic con-

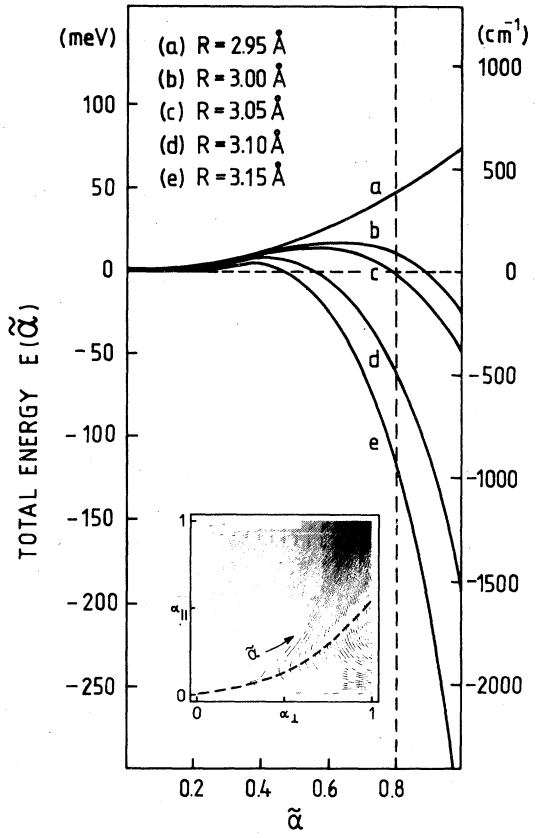

FIG. 4. Total energy of an exciton in an anisotropic elastic continuum calculated from Eq. (2) [with Eq. (5)] for different R values with the input parameters of Fig. 2 along the path indicated in the energy contour diagram of the inset (see also Ref. 18).

tinuum[1] to the case of an anisotropic continuum. The relation with the isotropic case becomes apparent by considering the total energy of Eq. (2) [with Eq. (5)] along the path indicated in the inset of Fig. 4. The total energy $E(\tilde{\alpha})$ shows two types of minima: The minimum $E(\tilde{\alpha}=0)=0$ represents the delocalized free-exciton state $[\psi(\vec{r})=\text{const}]$ and is separated by a potential barrier from the minimum at $\tilde{\alpha}\simeq 1$, which corresponds to a STE state with a strongly localized envelope. This situation is in agreement with the experimental observation of emission from both states. For decreasing R the STE is destabilized and eventually ceases to exist in accordance with the vanishing of the $\vec{E}\perp c$ emission from the localized state (Fig. 3).

The continuum model does not strictly determine the $\tilde{\alpha}$ value corresponding to an envelope function, which is localized to about one lattice constant. It turns out that the energy difference between the free exciton and the STE at $\tilde{\alpha}=0.8$ in Fig. 4 is in quantitative agreement with the energy difference between the emission data for $\vec{E}||c$ and $\vec{E}\perp c$ in Fig. 3.

In conclusion, we interpret optical emission data for the quasi-one-dimensional semiconductor $Mg[Pt(CN)_4]\cdot 7H_2O$ under hydrostatic pressure using band calculations and continuum models for free and self-trapped excitons. The quantitative agreement between experimental and theoretical data (Fig. 3) gives support to the interpretation that a self-trapped exciton is destabilized due to the pressure-induced change of the intrinsic material parameters.

[1]T. Toyozawa, in *Proceedings of the 1979 Toniguchi Symposium on Relaxation of Elementary Excitations,* edited by R. Kubo and E. Hanamura (Springer, New York, 1980), p. 3; in *Vacuum Ultraviolet Radiation Physics,* edited by E. E. Koch, R. Haensel, and C. Kunz (Pergamon, Braunschweig, 1974), p. 317; D. Emin and T. Holstein, Phys. Rev. Lett. 36, 323 (1976).

[2]W. Holzapfel, H. Yersin, and G. Gliemann, Z. Kristallogr. 157, 47 (1981).

[3]Y. Hara, I. Shirotani, Y. Ohashi, K. Asaumi, and S. Minomura, Bull. Chem. Soc. Jpn. 48, 403 (1975).

[4]The metallic member of this family is KCP ($K_2[Pt(CN)_4]Br_{0.3}3H_2O$) with $R=2.89$ Å, whose metallic properties are due to the nonstochiometric Br.

[5]M. Stock and H. Yersin, Solid State Commun. 27, 1305 (1978); H. Yersin, I. Hidvegi, G. Gliemann, and M. Stock, Phys. Rev. B 19, 177 (1979).

[6]H. Yersin and G. Gliemann, Ann. N.Y. Acad. Sci. 313, 539 (1978).

[7]H. Yersin, Habilitations-Schrift, Universität, Regensburg, 1979, (unpublished).

[8]P. Day, J. Am. Chem. Soc. 97, 1588 (1975).

[9]L. V. Interrante and R. P. Messmer, in *Extended Interactions between Metal Ions in Transition Metal Complexes,* edited by L. V. Interrante (American Chemical Society, Washington D. C., 1974), p. 382.

[10]R. P. Messmer and D. R. Salahub, Phys. Rev. Lett. 35, 533 (1975).

[11]H. Yersin, G. Gliemann, and U. Rössler, Solid State Commun. 21, 915 (1977).

[12]W. v. Ammon, H. Yersin, and G. Gliemann, Nuovo Cimento B 63, 3 (1981); H. Yersin and M. Stock, J. Chem. Phys. 76, 2136 (1982).

[13]M. Eichhorn, F. Willig, and H. Yersin, Chem. Phys. Lett. 81, 371 (1981).

[14]W. Holzapfel, H. Yersin, and G. Gliemann, J. Chem. Phys. 74, 2124 (1981).
[15]I. Hidvegi, W. v. Ammon, and G. Gliemann, J. Chem. Phys. 76, 4361 (1982).
[16]E. W. Montroll, J. Phys. Soc. Jpn. 26, Suppl. 6 (1969).
[17]B. Pertzsch and U. Rössler, Phys. Status Solidi B 101, 197 (1980).
[18]B. Pertzsch and U. Rössler, Solid State Commun. 37, 931 (1981).
[19]G. Weiser and L. Sebastian (unpublished).